T2R2 東京科学大学 リサーチリポジトリ
Science Tokyo Research Repository

論文 / 著書情報
Article / Book Information

Title	Blade-type Crawler Vehicle with Wings in Ground Effect for Traversing Uneven Terrain at High Speed
Authors	Yasuyuki Yamada, Gen Endo, Taro Nakamura
Citation	Proc. of The 2016 IEEE/RSJ International Conference on Intelligent Robots and Systems, , , pp. 3575-3580
Pub. date	2016, 10
Copyright	(c) 2016 IEEE. Personal use of this material is permitted. Permission from IEEE must be obtained for all other uses, in any current or future media, including reprinting/republishing this material for advertising or promotional purposes, creating new collective works, for resale or redistribution to servers or lists, or reuse of any copyrighted component of this work in other works.
DOI	http://dx.doi.org/10.1109/IROS.2016.7759526
Note	This file is author (final) version.

Powered by T2R2 (Science Tokyo Research Repository)

Blade-type Crawler Vehicle with Wings in Ground Effect for Traversing Uneven Terrain at High Speed

Yasuyuki Yamada[1],*Member, IEEE*, Gen Endo[2],*Member, IEEE* and Taro Nakamura[1],*Member, IEEE*

***Abstract*—Unmanned rescue, observation and/or research vehicles with high terrain adaptability, high speed, and high reliability are needed to reach difficult locations. However, most vehicles achieve improved performance over rough terrain at the expense of low speed and/or complex mechanisms. We developed a blade-type crawler robot with a very simple and reliable mechanism, capable of traversing uneven terrain at high speed, using aerodynamic devices. As these small devices are in the low Reynolds number region, we tested a wing that made use of the ground effect. We experimentally confirmed the success of this approach in improving the traveling speed and ability to traverse uneven terrain. The robot with aerodynamic lift was climbed 1.5 times higher obstacle than without wings.**

I. Introduction

Several robots are developed for traversing rough terrain, such as rescue and observation robots. These are used in place of humans to carry out data collection and other operations in locations that are dangerous or difficult for people to enter [1]. Many studies have focused on improving the mobility of such robots by compromising on other features. These robots are also expensive, limiting the situations wherein they are deployed. In this study, we attempted to design a simple and inexpensive system configuration to improve robot mobility over rough terrain without lowering the speed and/or requiring complex controls. A blade-type crawler was developed (Fig.1 (a)), wherein blades were mounted around a crawler belt, making contact with the ground and acting both as legs and as a suspension mechanism. The crawler robot was field tested on Mount Mihara on Izu Oshima Island and demonstrated superior performance and speed over rough terrain, compared with a conventional crawler [2]. We further proposed a small robot with a blade-type crawler adapted to high-speed travel in narrow and uneven rough terrain (Fig.1 (b)). A maximum speed of 2.1 m/s was achieved, and obstacles 3.5 times higher than the height of the vehicle were surmounted [3]. The study aimed to develop a small-sized robot with both increased rough terrain adaptability and a higher traveling speed. To achieve a higher speed, high power thrust and light weight are necessary, but this may incur other penalties such as vibration of the body and/or slipping on the ground surface. To address these problems, aerodynamic devices and/or damping devices have proven to be effective.

For example, Fig. 2 shows the use of aerodynamic wings (Fig. 2(a)), cancellation of vibration by using a mass damper (Fig. 2(b)), and stabilizing the body by increasing the body inertia (Fig. 2(c)). However, the robot's small size means that it has a low Reynolds number; hence, its aerodynamic characteristics are different from, for example, those of a passenger car. Small robots with aerodynamic devices have previously been demonstrated, including DASH+Wings [4] and VelociRoACH [5]. These are small hexapedal winged robots that use flapping wings to increase the locomotion capabilities. In this study, we develop a blade-type crawler robot with aerodynamic features. We will address the use of mass dampers and extra inertia in future studies. We focused on the use of the ground effect to gain aerodynamic efficiency in the low Reynolds number region. In addition, for leg locomotion robots (at least blade type crawler robot), there is no precedent to help decide whether the lift or downforce is the more effective. Hence we tested both aerodynamic lift and down force. The effectiveness of this approach on uneven terrain at high traveling speeds and climbing obstacles were experimentally confirmed.

(a) Blade-type crawler on the desert of Izu Oshima Island

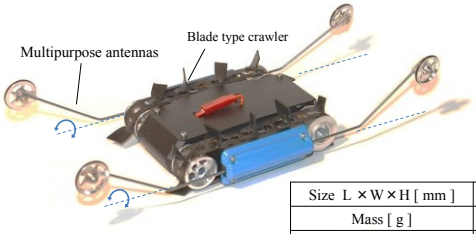

Size L × W × H [mm]	265 × 99 × 26
Mass [g]	255
Degree of Freedom	3

(b) KEIOS-I

Fig. 1 Blade-type crawlers

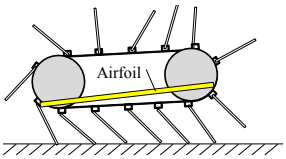

(a) Aerodynamics

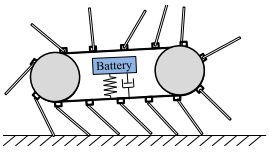

(b) Mass damper

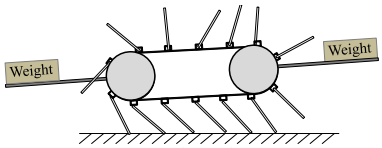

(c) Balance bar

Fig. 2 Devices for high speed running on rough terrain

[1]Yasuyuki Yamada and Taro Nakamura are with the Faculty of Science and Engineering, Chuo University 1-13-27 Kasuga, Bunkyo-ku, Tokyo 112-8551, Japan (yamada156 (at) 2009.jukuin.keio.ac.jp).

[2]Gen Endo is with the Department of Mechanical and Aerospace Engineering, Tokyo Institute of Technology, 2-12-1Ookayama, Meguro-ku, Tokyo, 152-8552, Japan.

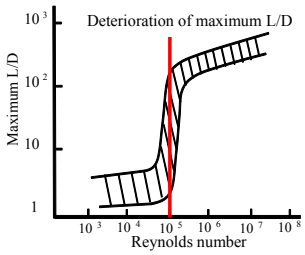

Fig. 3 Relation between L/D and Re [7]

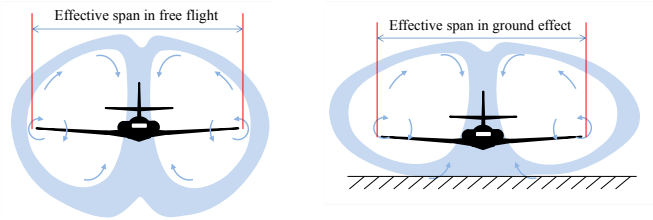

(a) In free flight (b) Close to ground

Fig. 4 Ground effect

II. Aerodynamics of Small Robots and Ground Effects

To improve the rough terrain drivability of small devices, it is necessary to consider the effects of scale, such as size and weight. The dominant dimensionless quantity is the Reynolds number. As the size becomes smaller, the surface to volume ratio increases. For example, basilisk lizards, which weigh about 2–200 g, can run across a water surface on their hind legs. The thrust is related to the surface of the foot, and the weight is related to the body volume. A 2 g lizard can achieve a 225 % thrust, which is enough to support its own weight. In contrast, a 200 g lizard can achieve only 111% thrust, which is only just enough to support its own weight [6]. A robot using the same effect as the basilisk lizard is therefore limited to a range of approximately 2–200 g. Similarly, a blade type crawler is effective in a size range of about 0.05 to 0.3 m, as demonstrated in our previous studies [2][3]. At this size and running velocity, the Reynolds number is low. The maximum speed of the KEIOS-I is 2.1 m/s and its length L[m] is 0.12 m, giving an Re of about 1.7×10^4 from Equation (1), where ν: Kinematic viscosity coefficient (1.512×10^5 m²/s) and v is the velocity [m/s].

$$\mathrm{Re} = vL/\nu \tag{1}$$

As shown in Fig. 3, in the Re of the robot, the L/D, which expresses the relation between the lift and drag forces of the airfoil, is very small [7]. This means that at this Re region, the airfoil shape of a passenger aircraft may not be applicable. An aerodynamic device specified to this size of device was needed to improve the mobility of the blade type crawler. When the L/D is not low, high-lift devices are used. For example, methods wherein the exhaust from the engine flows to the wing are used in passenger planes. However, such devices are difficult to add to small robots, and devices must be specifically designed. We focused on the use of the ground effect to solve this problem. The ground effect is described in Fig. 4. In free flight (Fig. 4(a)), the effective span of the wings is limited to the wing span. However, when a wing approaches the ground two phenomena add to the lift force and reduce the drag, effectively increasing the wing span (Fig. 4(b)). Using the ground effect, a vehicle can get more lift from the same wing area. We used this in the design of an aerodynamic device to improve the mobility of a blade-type crawler over uneven terrain at high-speeds.

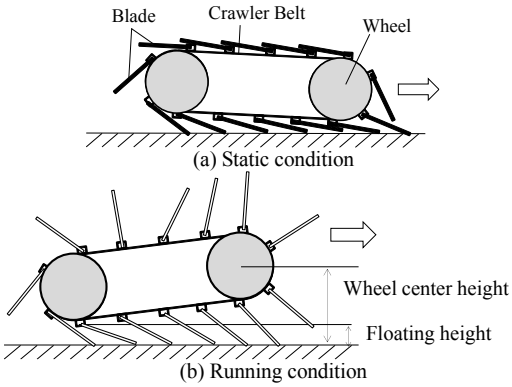

Fig. 5 Running methods of the blade-type crawler

III. Blade-Type Crawler

A. Mechanism of a Blade-Type Crawler

Typical approaches to moving robots over rough terrain include the leg-, wheel-, and crawler-type mechanisms. The aim of the mobile mechanism developed in this study was to improve both the traveling speed and the ability to traverse rough terrain. In general, the rough terrain performance of a leg-type mechanism is high, but the speed is low. Wheel-type mechanisms are characterized by high speed but low performance over rough terrain. The crawler-type mechanism provides a balance between the features. The crawler-type mechanism is therefore often used for rescue robots and was adopted in this study. We devised a crawler with blades mounted passively and flexibly on the crawler belt. Figure 1 shows an outline drawing of the mechanism. When the vehicle is moving slowly, as in Fig. 5(a), the overall height barely changes from the static height. During high-speed operation, as in Fig. 5(b), the blades open outward because of the centrifugal force of the wheels, and the wheel diameter is increased. When the blades are open and supporting the body, they make contact with the ground and act as legs. The stiffness of the blades was adjusted in such a way that all blades bend when there is no friction on the surface of the ground. [2] This produces a gap between the body of the vehicle and the ground and acts as a suspension mechanism, allowing the vehicle to traverse uneven ground efficiently.

B. Step mobility by the blade-type crawler

The blade-type crawler can ascend steps by lifting the robot with the blades at the rear end, as shown in Fig. 6. For a crawler to be able to climb over steps, the center of gravity of the robot must be above the extended line of the vertical wall of the step, assuming that the blades can flex in a direction tangential to the wheel. Here, h is the height of the step, L_G [m] is the distance from the center of gravity to the center of the rear wheel, r is the radius of the wheel, H_G [m] is the height of the center of gravity, a [°] is the angle of inclination of the robot, and l [m]is the length of the blade. The blade can lift the vehicle to a maximum height of h_b [m], which can be determined using Eq. (2):

$$h_b = \sqrt{r^2 + \ell^2} - r \tag{2}$$

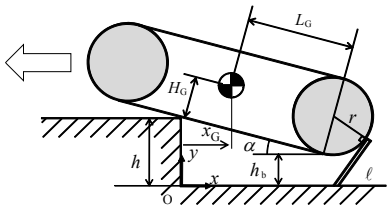

Fig. 6 Blade-type crawler moving over a step

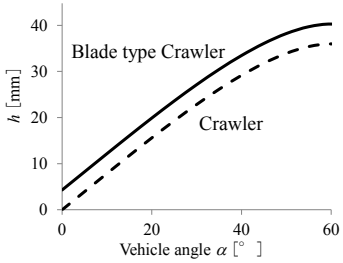

TABLE I: PARAMETER SETTINGS

L_G	45 mm
r	12 mm
H_G	10mm
l	15mm

Fig. 7 Height of the climbed steps

The x-coordinate of the center of gravity x_G [m] is expressed by Eq. (3):

$$x_G = \frac{h-\sqrt{r^2+\ell^2}+r}{\tan\alpha} - L_G\cos\alpha - r\tan\frac{\alpha}{2}\cos\alpha + H_G\sin\alpha \quad (3)$$

To enable movement over the step, the center of gravity of the x-coordinate should be negative, and therefore, Eq. (3) can be rewritten as Eq. (4), with $x_G = 0$.

$$h = L_G\sin\alpha + r\tan\frac{\alpha}{2}\sin\alpha - H_G\sin\alpha\tan\alpha + \sqrt{r^2+\ell^2} - r \quad (4)$$

The maximum height of step that can be climbed is obtained using this equation. The lifting height, h_b, of the rear wheels can be calculated using Eq. (2). The climbing capacity of an ordinary and a blade-type crawler, as well as the relation between the angles of inclination of the robot and the climbing heights, are shown in Fig. 7. Table 1 lists the robot parameters. The height of step that can be climbed is higher for a blade-type crawler, and when climbing steps of the same height, the angle of inclination of the robot can be reduced. The height limit of the step is about 40 mm for a blade-type crawler with a blade length of 15 m, compared with 35 mm for a robot without blades. This is an increase of about 14%, and does not take into account the dynamic movement or aerodynamics, which would further improve the performance of an actual robot.

IV. GROUND EFFECT FOR BLADE-TYPE CRAWLER

A. Overview of aerodynamic design for the robot

We developed a small blade-type crawler robot at low *Re* with the ability to traverse uneven terrain at high speed. When a blade-type crawler is running, the body is supported by the blades, producing leg-like locomotion, as shown in Fig. 8(a). When the robot is climbing a step or high obstacle, the blades of the rear crawler section are pushed up to act like rear legs. In the case of KEIOS-1 (Fig. 1(b)), the multipurpose antennas act like sub-crawler arms and allow the robot to climb 90 mm steps. These were set as the design criteria of our novel blade-type crawler robot. The weight of a blade-type crawler robot without wings or multipurpose antenna mechanism, is 95 g. At a certain velocity, the robot

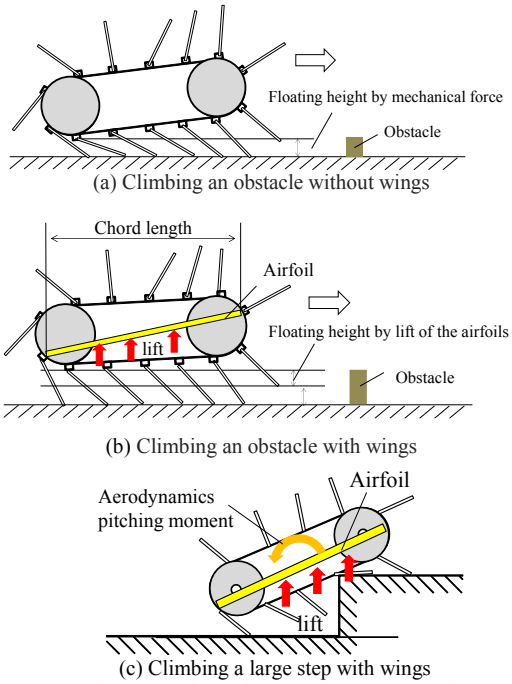

Fig. 8 Aerodynamic effect in uneven terrain

stops accelerating because the blades slip on the ground. Our goal was to maintain the uneven terrain drivability, while achieving high-speed runs. To confirm the performance over uneven terrain, the robot was tested taking large steps on a road with small continuous obstacles. Aerodynamic downforces are often used to keep a vehicle on the road. However, a running robot is floating above the ground, and there is no precedent to help decide whether the lift or downforce is the more effective.

It was expected that adding downforce would make the robot more stable in its posture and achieve greater grip and acceleration. On the other hand, the added lift would increase float and the ability to climb larger obstacles, as shown in Fig. 8(b), and also raise the front of robot and increase the pitching moment, as shown in Fig. 8(c), which expected to support the robot when climbing an obstacle. As a blade-type crawler can climb approximately 14 % higher than an ordinary crawler, the blade-type crawler + wing was expected to climb even larger obstacles.

B. Design of the wings

At low Re, special design is needed to achieve effective aerodynamic force. As shown in Fig 3, the Re 10^4 area has a small L/D ratio. Hence, if the aerodynamic force which supports the robot is achieved by a typical airfoil design, the drag force is expected to reduce both the acceleration and the maximum running speed. To decrease drag and increase lift (or downforce), a larger L/D ratio is needed. The factors considered included the shape of the wing, the angle of attack, and the wing mounting method. First, the shape of the wing was considered. Very few studies are available on airfoils of less than 10^4 in area. One reason is that the aerodynamic force is very small, making it difficult to measure accurately. A small airfoil with a complex curved surface is also difficult to make. However, a well-known aerial vehicle in this Re range is the paper airplane. The wing shape of a paper airplane is

flat, very thin, and easy to make. At the typical passenger airplane, the leading edge of the airfoil is rounded. However, when the leading edge of the airfoil of a paper airplane is made sharp, the L/D increases by about 20% [8]. A C_L of about 0.7 is expected with an angle of attack of 6°–10° [8].

Next, the ground effect was considered. The aspect ratio AR was used to compare the wing performance, using Eq. (5), where b [m] is the wing span, and S [m^2] is the wing surface:

$$AR = b^2 / S \tag{5}$$

The ground effect was predicted using AR and h/c ratios from past studies, where h [m] is the distance between the under surface of the wing and the ground surface, and c [m] is the chord length of the wing. When $AR = \infty$ or $AR = 6$ to 2, and when h/c changes from 1 to 0, the L/D ratio (ground effect) increases [9]. The c of the aerodynamic device of the robot had a maximum value of about 120 mm, as this was the length of the robot. At an h/c of about 0.1, the C_L was expected to be about three times larger than that in free flight [9]. In our robot, h was less than 12 mm. The side shape of the wing tip also affects the aerodynamics. As shown in Fig. 9, the wing tip sides were bent, to increase the effective wing span and L/D ratio using the ground effect. Figure 9(a) shows the side skirt and Fig. 9(b) the winglet. The side skirt is often used in race cars to achieve the ground clearance needed for the suspension mechanism, while the winglet is often used in passenger airplanes. In the case of a robot, there is no need to maintain the ground clearance, and reducing the wing surface height h allows larger aerodynamic forces to be achieved. Hence, we used winglets on the robot wings.

Next, the relation between the angle of attack and lift at this Re was considered. Using a NAXA0012 airfoil that has a relatively thin symmetrical shape, the C_L can be increased to an angle of attack of about 8°, beyond which the C_L is almost constant [10]. Hence, we set the angle of attack to about 8°–10°. This was expected to provide a stable aerodynamic force when the robot posture was changed while running.

The blade type crawler had a pitch angle of about 2°, as shown in Fig. 10. When setting the angle of attack, this angle must be taken into consideration, as shown in Fig. 11, where α [°] is the angle of pitch when the robot is running, β [°] is the mounting angle on the robot, and γ [°] is the angle of attack. Figure 11(a) shows the angle-setting method of the aerodynamic device to achieve lift force, and Fig. 11(b) the

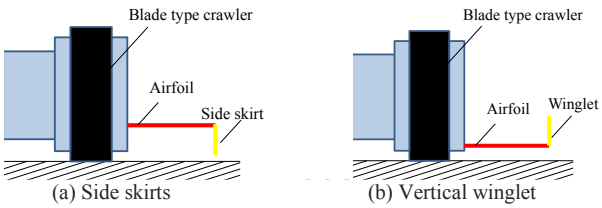

(a) Side skirts (b) Vertical winglet

Fig. 9 Wing tip shape

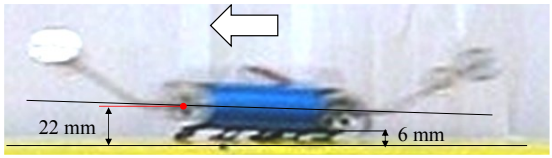

Fig. 10 Floating height of KEIOS-I

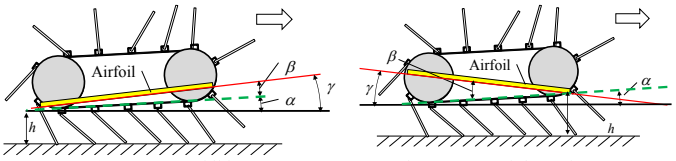

(a) In case of lift (b) In case of downforce

Fig. 11 Angle of attack

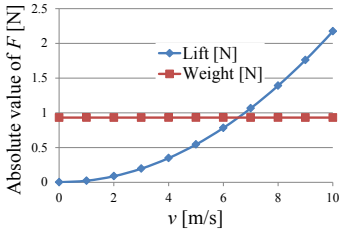

Fig. 12 Expected aerodynamics

angle setting method to achieve downforce. Finally, we estimated the aerodynamic effect. In the experimental device, the size of the side wing span was set to 50 mm, and the chord length was set to 0.12. The total wing surface S was 0.012 m^2, h[m] was set to 0.012 m, the ground effect coefficient k was expected to be 4, and the density of the air ρ was 1.293 kg/m^3. The running velocity of the robot was v [m/s] and C_L was estimated to be 0.7. The expected aerodynamic force F [N] was calculated using Eq. (6).

$$F_L = \frac{1}{2} k \rho V^2 S C_L \tag{6}$$

The relation between the absolute value of F and the running velocity v (m/s) is shown in Fig. 12. The robot weight was 95 g, so when the running velocity of the robot was greater than 6.6 m/s, the aerodynamic force was expected to exceed the weight of the robot. At the 2.1 m/s maximum speed of KEIOS-1, the aerodynamic force was more than 10% of the weight of the robot, and was expected to affect the running behavior. Aerodynamic effects are nonlinear, hence wind tunnel experiments using running robots are needed. This requires a special treadmill system and will study in future.

V. Development of KEIOS- II

In this section, we describe the development of the KEIOS-II, a blade-type crawler with an aerodynamic device. The KEIOS- II is shown in Fig. 13. The total length was 120 mm, and the crawler section length was 115 mm. The blade length of the crawler was 15 mm, and the width was 10 mm.The robot had a symmetrical body shape both from front to rear and top to bottom. The drive wheels were driven by a brushless motor and a 7.4 V × 220 mAh Li-Po battery was mounted on the bottom of the body. The reduction ratio was 5.37:1, and the total weight was 95 g. The wings were made from 0.5-mm-thick polycarbonate sheets. They were 120 mm in length and 50 mm in width and attached at an angle γ of about 10° to the ground. Both ends of the wing had a winglet shape, and the front edges were sharpened to achieve a better L/D ratio. The wings were mounted 8 mm from the ground to achieve the ground effect. The crawler belts were arranged on the left and right sides of the vehicle with 11 blades attached at 25 mm intervals to each crawler. The blades were rubber plates with 1 mm thickness and were connected to the crawlers. The number of blades, materials used, and shape of

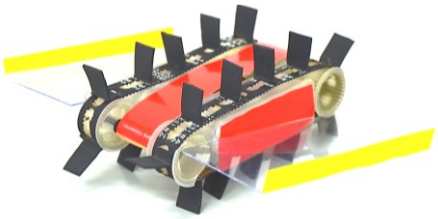

Fig. 13 KEIOS-II

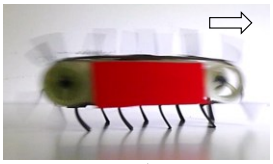

(a) Without wing （1m/s or less)

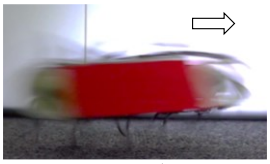

(b) Without wing （2m/s or more)

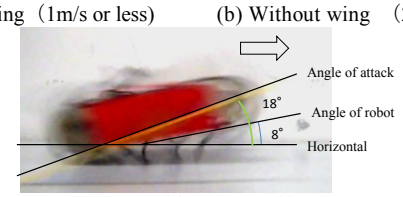

(c) With wing (Lift)

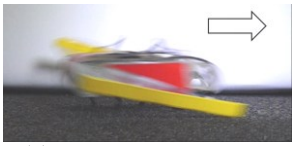

（d） With wing (Downforce)

Fig. 14 Angle and height of the vehicle when running

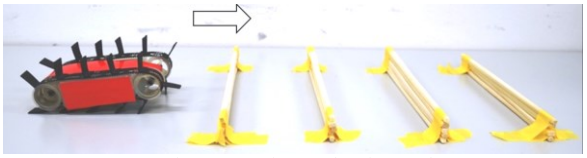

Fig. 15 Continuous barrier road

TABLE II. THE RESULT OF MAX SPEED TEST

The condition	MAX speed (m/s)
+10 °wing	3.5
No wing	3.1
−10 °wing	2.9

TABLE III. THE RESULT OF DRIVABILITY ON CONTINUOUS STEP TEST

The condition	MAX hight of continous steps (mm)
+10 °wing	30
No wing	20
−10 °wing	10

TABLE IV. THE RESULT OF THE LARGE STEP CLIMBING TEST

The condition	MAX Step hight (mm)
+10 °wing	60
No wing	40
−10 °wing	10

the KEIOS-II were based on previous experience of designing blade-type crawler robot [3]. In this study, in order to confirm the effect of Aerodynamics device, these were mounted on the left and right of the robot. In the future, the shape of robot body itself will change to an aerodynamics design.

VI. EXPERIMENT

Experiments were conducted to test the use of a wing with ground effect on uneven terrain at high speeds. We compared the robot under three conditions: 1) without wings, 2) with β = +10° wings (adding lift), and 3) with β = −10° wings (adding downforce). Three type tests were conducted to verify 1) The maximum running velocity, 2) the performance when running across continuous barriers, and 3) the performance in step climbing. Test 1 measured the maximum running velocity. The robots ran a 2 m section and were recorded using a camera. The maximum velocity was calculated by the times. The results of Test 1 are shown in Table 2. The fastest speed was recorded with the β = +10° wing, and the second fastest was recorded with no wing. This is different from passenger cars. The fastest speed was recorded when the grounded load of the crawler was lowest. The running states were as shown in Fig. 14. In case of with no wing were as shown in Fig. 14(a) and (b). At about 1m/s, the pitching angle of robot was about 0° (Horizontal). At about 2m/s, the pitching angle of robot was about 2°. In contrast, with the β = +10° wing was as shown in Fig. 14(c). The robot with the β = +10° wing was at the greatest angle of inclination, whereas the robot with the β = −10° wing was not inclined by the downforce as shown in Fig. 14(c). We expected to find the fastest condition when the contact area was widest, however the result was the exact opposite: although the robot with the β = +10° wing had the smallest contact load and area, the grounded pressure was larger and the rolling resistance of the crawler was the lowest found. In contrast, the contact area of the robot with the β = −10° wing was largest, and the rolling resistance was also the largest found, due to the effect of the downforce. In case of -10°wing, the crawlers were pressed by the down force. The grip was increased and at the same time, rolling (running) resistance of crawlers were increased. Hence it overall became slower than the normal. On the other hand, in case of + 10°wing, the up-force affected to both grip and the resistance decrease. In addition, we estimate that reaction rate of grip is less than reduction rate of resistance. Hence it overall became faster than the normal. The maximum speed recorded with an aerodynamic device fitted was about 3.5 m/s. In this case, *Re* is about 2.8×10^4 from Equation (1). Test 2 compared the ability to traverse continuous barriers, as shown in Fig. 15. Barriers 5 mm in width were placed at 100 mm intervals. The height of the barriers increased by 5 mm. We recorded the highest barrier that each robot was able to traverse. The results are shown in Table 3. The robot with a β = +10° wing performed best, surmounting barriers 30 mm in height in continuous steps, compared with 20 mm for the robots without a wing. The state of each robot when crossing the barrier is shown in Fig. 16. In the case without wings, at heights over 20 mm the robot was unstable, and subject to large pitching and falling, as shown in Fig. 16(a). In contrast, with β = +10° wings, the robot was stable and the pitching movement was reduced, as shown in Fig. 16(b). As the inertia and weight of the wing was very small. Pitch inertia of the aerodynamics device is less than 4% of the pitching inertia of the robot. Hence, any difference was the result of aerodynamic effects. Test 3 compared the ability to climb a large obstacle. We recorded the maximum height achieved by each robot. The results are shown in Table 4. The robot with +10° wings climbed highest, while the robot with −10° wings showed the lowest obstacle climbing ability. Figure 17 shows the state of the robots when climbing the obstacle. The robot with +10° wing climbed 1.5 times higher than the robot without wings, because of the aerodynamic support. When the front of the

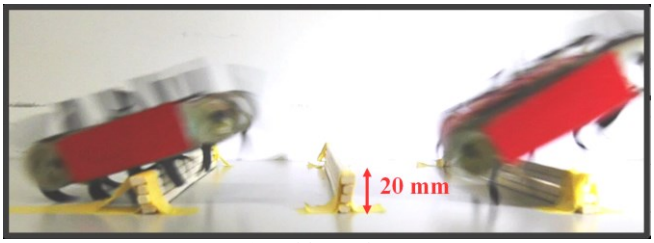

(a) Without wings

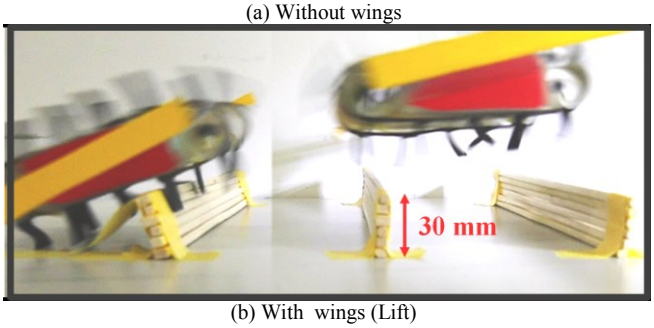

(b) With wings (Lift)

Fig. 16 Running over continuous barriers

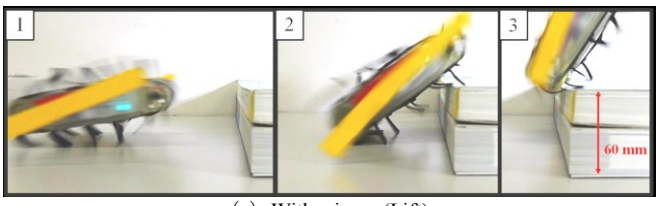

(a) With wing (Lift)

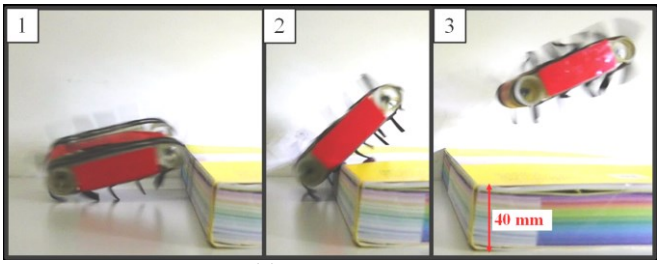

(b) With no wing

Fig. 17 Climbing a large obstacle

robot contacted the obstacle and became inclined, the angle of attack increased and it makes the pitching moment. It was speculated that this moment supported to climb the obstacle, as shown in Fig. 17(a). In contrast, when the front of the robot with −10° wings contacted the obstacle, it was speculated that the downforce inhibited to change the angle of inclination of the robot. And, the front edge of -10° wings were often caught on the obstacle, inhibited to climb too. In addition, as shown in Fig. 17(b), with no wing, the climbed height was 40 mm that meet the height expected in section 3. The results showed that the KEIOS- II with wings could climb up to 2.6 times its own height. We conclude that the use of a $\beta = +10°$ wing to add lift improved the blade-type crawler robot's mobility in this experiments condition. The lift provided by aerodynamics made the robot adopt a more inclined position during running as shown in Fig. 14(c), which increased its maximum speed, ability to traverse continuous barriers, and obstacle climbing. However, these experiments were conducted under very limited circumstances, for example taking no account of wind impact.

VII. Conclusions

This study presented the KEIOS-II, a small unmanned vehicle intended to deliver high performance over rough terrain and at high speed. By attaching an aerodynamic device that efficiently delivered aerodynamic force even in the low Re area, the performance over uneven terrain in high-speed traveling improved. The following results were achieved:

1. The maximum speed was 3.5 m/s.
2. An obstacle 2.6 times greater than the height of the robot was climbed by aerodynamics assist.
3. The robot with aerodynamics devices was climbed 1.5 times higher obstacle than without wings.
4. The lift provided by aerodynamics increased its maximum speed, ability to traverse continuous barriers, and obstacle climbing.

Thus, the KEIOS-II demonstrated high performance over rough terrain and high speed movement, despite being a small vehicle. In the future, we plan to conduct wind tunnel experiments using a treadmill system.

References

[1] S. Odedra, S. D. Prior, and M. Karamanoglu, "Investigating the Mobility of Unmanned Ground Vehicles," *Proceedings of International Conference on Manufacturing and Engineering Systems*, 2009, pp.380–385.

[2] Yasuyuki Yamada, Miyagawa Yutaka, Ryota Yokoto and Gen Endo, "Development of a Blade-type Crawler Mechanism for a Fast Deployment Task to Observe Eruptions on Mt. Mihara," *Journal of Field Robotics*, 2015.

[3] Yasuyuki Yamada, Gen Endo and Edwardo F. Fukushima, "Blade-Type Crawler Vehicle Bio Inspired by a Wharf Roach," *ICRA 2014*, Hong Kong, China, 2014.

[4] K. Peterson, P. Birkmeyer, R. Dudley, R. S. Fearing, "A wing-assisted running robot and implications for avian flight evolution," *Bioinspiration and Biomimetics*, October 18, 2011, 6, 046008

[5] Duncan W. Haldane, Kevin C. Peterson, Fernando L. Garcia Bermudez, and Ronald S. Fearing, "Animal-inspired Design and Aerodynamic Stabilization of a Hexapedal Millirobot," *IEEE ICRA* May 2013, pp. 3279–3286

[6] J Glasheen, T Mcmahon, "Size-dependence of water-running ability in basilisk lizards (Basiliscus basiliscus)," *Journal of Experimental Biology*, vol. 199, 1996, pp.2611–2618 .

[7] Viieru D. Tang, J. Lian, Y. Liu, H. and Shyy W., "Flapping and flexible wing aerodynamics of low Reynolds number flight vehicles," *44th AIAA Aerospace Science Meeting and Exhibit*. 2006.

[8] Kanichiro Kato, "Effect of Tail Wing Area on Model Airplane Endurance Performance," *Journal of the Japan Society for Aeronautical and Space Sciences*, vol. 40, 1992, No. 461

[9] J. Katz, *J. Fluids Eng* 107(4), 438–443 (Dec 01, 1985) (6 pages)doi:10.1115/1.3242507History: Received May 04, 1984; Online October 26, 2009)

[10] Race Car Aerodynamics: Designing for Speed (Engineering and Performance), J. Katz, Bentley Publishers, 1996, pp. 93.